Antimatter, Annihilation, and the Stability Filter: Predictions for the CERN Antihydrogen Programme

Vijay Shankar Sharma

Independent Researcher, Gurugram, National Capital Region, India

vss@vijayshankarsharma.com | ORCID: 0009-0001-9622-6121

DOI: 10.5281/zenodo.20201014

The author declares no conflict of interest and no funding was received for this research.

Abstract

The CERN antihydrogen programme pursues three stated scientific goals: testing CPT symmetry between matter and antimatter to unprecedented precision, measuring whether antimatter falls under gravity identically to matter, and finding the physical origin of the matter-antimatter asymmetry of the observable universe. This paper states what the Big Flare-Up Theory (BFUT) framework predicts for each of these three goals, and explains why the third goal will not be achieved through antihydrogen spectroscopy alone.

The BFUT account of antimatter derives from BFUT Paper 16 (P16 [1]), which establishes that approximately 97% of quark-class excitation parameter space produces the stable 3+e topology (full five-term functional; four-term baseline 85%) that becomes matter, while the remaining approximately 3% produces unstable excitations that generate their own equal and opposite substrate rebound at the moment of formation. That rebound is the antiparticle. The matter-antimatter asymmetry of the observable universe is therefore not a mystery requiring an unexplained asymmetric process. It is the direct output of the stability filter operating at quark-class formation level. Four specific falsifiable predictions are stated for the CERN programme.

The predictions arise from the physical matter substrate that the author names the Spaticle field. Paper 16 derives the equilibrium density as $\rho_s = 7.3 \times 10^{-27}$ kg/m^3. The same condensation framework supplies the stability analysis and the structural inputs used here. Particle-sector electroweak quantities are derived in P19 from the condensation functional and proton-scale

anchors. This paper applies that framework to antimatter, annihilation, and the CERN antihydrogen programme.

Keywords: antimatter; antihydrogen; CERN; ALPHA; matter-antimatter asymmetry; annihilation; Spaticle field; BFUT; stability filter; cancellation wave; CPT symmetry; equivalence principle

1. Introduction: The Standard Model's Three Open Antimatter Questions

BFUT identifies the Spaticle field as a physical matter substrate with equilibrium density $\rho_s = 7.3 \times 10^{-27}$ kg/m^3, obtained within the BFUT condensation framework in Paper 16 [1]. The matter substrate corresponds physically to what general relativity describes geometrically as spacetime. Because it has density, it bends, compresses, waves, and becomes entrained by organised matter. BFUT P14 develops the cross-programme substrate account [2], and BFUT L1 states its cosmological context [3].

The Spaticle field is not the luminiferous ether. The Michelson-Morley experiment excluded a preferred-drift background through which light propagates while matter exists separately. In BFUT, light and matter are excitations or condensations of the same Spaticle field. Light is a propagating disturbance of the substrate, and c is the substrate maximum reorganisation rate. All measuring instruments and measured signals are made from the same substrate, so uniform substrate-wide drift cannot be detected internally. The null result is compatible with this common-substrate model and does not distinguish the absence of a substrate from a substrate in which matter and light share the same carrier. Paper 16 gives the full argument [1]. Paper 17, Section 6.6, and Paper 19, Section 13, develop light as a substrate excitation [8][10].

The standard model of particle physics and standard cosmology together face three unresolved questions about antimatter that the CERN antihydrogen programme is specifically designed to address.

Question 1: CPT symmetry. The CPT theorem states that the laws of physics must be identical for a particle and its antiparticle when charge, parity, and time are simultaneously reversed. This has never been directly tested for antihydrogen at high precision. If CPT were violated, it would challenge the foundations of quantum field theory.

Question 2: Gravity on antimatter. General relativity predicts that antimatter falls under gravity identically to matter. This was untested directly until 2023. The weak equivalence principle requires confirmation for antimatter.

Question 3: The matter-antimatter asymmetry. The standard model predicts that the early universe produced equal amounts of matter and antimatter. The observable universe is overwhelmingly dominated by matter. The physical reason for this asymmetry remains unknown. The standard model requires CP violation beyond what is currently measured to account for it, and no complete explanation exists.

The BFUT framework addresses all three questions. It predicts the same answer as the standard model for Questions 1 and 2, and provides a different physical account of Question 3.

The predictions follow from the BFUT substrate condensation framework summarised in Section 3. The antimatter account is one component of the same structure that generates the force, particle, quantum, and gravitational relations used in the paper.

2. The CERN Antihydrogen Programme: What Has Been Done and What Is Planned

CERN operates the Antiproton Decelerator (AD) facility, which produces antiprotons by directing high-energy protons onto a metal target and decelerating the resulting antiprotons for experimental use. The ALPHA, ALPHA-g, AEgIS, GBAR, and BASE experiments all operate at the AD facility. The BASE experiment has measured the antiproton-to-proton charge-to-mass ratio at a precision of 16 parts per trillion [4].

Production and storage. The ALPHA experiment creates and magnetically confines antihydrogen for spectroscopic and gravitational measurements [5][6][7].

CPT results to date. The 1S-2S transition in antihydrogen was observed and found consistent with hydrogen at a relative precision of about 2×10^{-12} [5]. Later work characterised the hyperfine components of the transition [14]. In 2026, ALPHA reported a 4 ppm measurement of the ground-state hyperfine splitting [16]. No CPT violation has been observed in these measurements.

Gravity result (2023). The ALPHA-g experiment published the first direct measurement of the gravitational behaviour of antihydrogen in 2023 [7]. Antihydrogen was found to be gravitationally attracted to the Earth, falling downward, at a precision of approximately 20%. The result is consistent with the weak equivalence principle.

Planned programme. The CERN antihydrogen experiments continue to improve spectroscopic and gravitational tests.

Antihydrogen used in these experiments is produced and confined in the laboratory.

3. The BFUT Framework: Relevant Results for Particle Physics and Quantum Mechanics

Before addressing the BFUT account of antimatter specifically, it is useful to note what other papers in the BFUT programme establish at the particle physics and quantum mechanics level, since the antimatter derivation connects directly to these results.

BFUT Paper 17 (P17 [8]) derives the four fundamental forces sequentially from Spaticle substrate mechanics. The electromagnetic force emerges from the persistent internal circulation asymmetry of the 3+e condensation established in P16 [1]. The strong force arises from inter-condensation binding. The weak force arises from topology reconfiguration events. Gravity arises from substrate deformation. None of these forces is postulated independently. Each is a consequence of the substrate threshold topology.

4. Half-Integer Spin, H-Class Radial Physics, and Configuration Resonances

The results below connect directly to the matter-emergence model because they use the same condensation topology that generates the stability filter, cancellation wave, and CERN predictions developed later in this paper.

Half-integer spin from substrate topology. Standard quantum mechanics represents half-integer spin through Lorentz-group spinors. BFUT Paper 19A derives the fermionic value geometrically from the 3+e topology of P16 [1]. The bifurcation produces a condensation whose internal circulation returns to its initial configuration after two full rotations of the reference frame. This 720-degree restoration supplies the factor of 2 associated with spin 1/2. Within this construction, the result follows from the same threshold topology that produces the stability filter and cancellation wave.

H-class radial resonance from substrate geometry. The observed Higgs-class resonance is the electroweak-normalised radial resonance of the single Spaticle field. From the P16 condensation functional, A = 1/2 and the equilibrium radius is $R_0 = 1.27348221$. P19 defines the normalized electroweak radial coupling as

$$\lambda\_H\_vss = 2AR_0/\pi^2 = R_0/\pi^2 = 0.12903; \quad v\_vss = 6E\_unit/\alpha\_vss = 245.565\text{ GeV}; \quad m\_H\_vss = v\_vss\sqrt{(2\lambda\_H\_vss)} = 124.75\text{ GeV}/c^2.$$

This radial-resonance derivation follows from the same condensation architecture used throughout BFUT. The raw radial curvature $E''(R_0) \approx 3.2352$ and the normalized electroweak radial coupling λ_H_vss describe distinct quantities. The H-class mass follows from λ_H_vss and v_vss within the radial sector.

Configuration resonances of the four-unit condensation. The P16 four-unit functional has three evaluated configurations. The selected persistent topology is 3+1. The 2+2 and 4+0 configurations are higher excitations of the already-formed four-unit condensation.

$E(3+1) = 1.40$; $E(2+2) = 4.00$; $E(4+0) = 6.10$.

The excitation gaps from the selected minimum are

$\Delta E_{2+2} = E(2+2) - E(3+1) = 4.00 - 1.40 = 2.60$

$\Delta E_{4+0} = E(4+0) - E(3+1) = 6.10 - 1.40 = 4.70$

Using the P16 condensation energy unit

$E\_unit = m_p c^2/\pi = 298.661$ MeV,

the corresponding configuration-resonance energies are

$m\_Shankar\ c^2 = \Delta E_{2+2}\ E\_unit = 2.60 \times 298.661$ MeV $= 776.5$ MeV

$m\_BFUT\ c^2 = \Delta E_{4+0}\ E\_unit = 4.70 \times 298.661$ MeV $= 1403.7$ MeV.

Shankar resonance. The Shankar resonance is the 2+2 partition: two co-rotating pairs with net circulation $\Sigma s = 0$. Its natural relaxation divides the excited configuration into two light units; in the first generation this gives a two-pion channel.

BFUT resonance. The BFUT resonance is the 4+0 partition: all four units co-rotate with $\Sigma s = 4$. Relaxation toward the persistent 3+1 topology proceeds through emission of one light unit while leaving a correlated three-unit remnant, giving first-generation emission-plus-remnant channels including $\rho\pi$ and 3π-class final states.

Experimental resonance correspondence. The Shankar prediction $m\_Shankar\ c^2 = 776.5$ MeV lies at the $\rho(770)$ resonance: the listed neutral mass is 775.26 ± 0.23 MeV [17], a difference of 1.2 MeV (0.16%), and the dominant decay is $\pi\pi$. The BFUT prediction $m\_BFUT\ c^2 = 1403.7$ MeV lies in the 1.4 GeV resonance band. The first-generation emission-plus-remnant topology corresponds to light unflavoured channels in this band, including the $\omega(1420) \to \rho\pi$ channel. Strange-sector states are not required by the P16 construction.

The two resonance energies are direct outputs of the same four-unit condensation functional that selects the persistent 3+1 matter topology.

BFUT Paper 19 [10] derives particle-sector quantities from the P16 condensation structure and proton-scale anchors. The electroweak chain is independent: $m\_Z\_vss = \pi^4 m_p = 91.396$ GeV/c^2; P16 supplies $M = m_p/3$ and $n^2 = 16$, and P19 gives $m\_W\_vss = 256M = (256/3)m_p = 80.066$ GeV/c^2. Only after both masses are obtained independently is the BFUT weak mixing quantity calculated:

$\sin^2\theta$_W_vss = 1 − (m_W_vss/m_Z_vss)^2 = 1 − $256^2/(9\pi^8)$ = 0.23257. The H-class radial resonance is derived separately from λ_H_vss = R_0/π^2 and v_vss = 6E_unit/α_vss.

BFUT Paper 19A (P19A [9]) develops quantum-mechanical foundations from the Spaticle substrate, including the half-integer-spin construction and related quantum interpretations. BFUT has one Spaticle field, and the observed H-class state is its electroweak-normalised radial resonance. The Shankar and BFUT configuration resonances are derived in this paper from the P16 four-unit excitation structure and are independent of the antimatter stability-filter mechanism.

BFUT Paper 18 [11] gives the carrier equation $\Psi(r,t) = -(GM/r)\exp(-r/R_{eff})\, R(\tau\_c, \partial\_t)\, N(\Sigma_i)$. It defines $R_d = [3M/(8\pi\rho_s)]^{1/3}$ and $R_{eff} = R_d(1 + v\_rot^2/c^2)^{1/3}$. The factor $8\pi G$ is physical in this construction: the Spaticle field is the matter substrate corresponding to what general relativity describes geometrically as spacetime, and it bends, compresses, waves, and becomes entrained because it has density. The same density gives $a_s = c\sqrt{(G\rho_s/3)}$. The current SPARC results report 92.0% shape agreement, 98.8% flat classification, and a median outer relative residual of 0.096; the KiDS-1000 isolated-lens comparison uses the same a_s. Rotational entrainment supplies the additional outer-galaxy support.

These connected papers use the same substrate density and condensation structure across particle physics, quantum mechanics, and gravitation. In this paper, only the parts needed for the antimatter mechanism and its experimental predictions are used.

The BFUT framework is therefore a quantitative and experimentally testable programme. The particle physics results above provide the context within which the antimatter account below should be read.

5. The H-Class Radial Resonance of the Spaticle Field

The experimentally observed Higgs-class resonance is retained as the electroweak comparison state. In BFUT, however, the ontology contains one Spaticle field. The H-class state is a radial resonance of that field; BFUT does not introduce a second Higgs field that supplies the W and Z masses.

The BFUT claim is therefore specific: electroweak phenomenology conventionally represented through a Higgs scalar sector is represented in BFUT by radial dynamics of the single Spaticle field. This does not make the mixing quantity a parent of the W or Z masses. P19 derives the neutral and charged resonances independently and obtains the mixing quantity only afterward from their squared mass ratio.

The H-class chain is λ_H_vss = $2AR_0/\pi^2$ = R_0/π^2, v_vss = 6E_unit/α_vss, and m_H_vss = v_vss$\sqrt{(2\lambda_H_vss)}$ = 124.75 GeV/c^2. Here E_unit = m_pc^2/π. The H-class result therefore follows from the P16/P19 radial condensation structure and does not use Ψ_vac, the top-quark mass, m_W_vss, m_Z_vss, or $\sin^2\theta$_W_vss as inputs.

In BFUT, particles are stable condensations of the Spaticle matter substrate. Their mass is the energy required to maintain the condensation structure: the localisation term A/R^2, displacement term BR^2, and boundary term CR in the P16 [1] free-energy functional. The bosonic masses arise from substrate reconfiguration modes with intrinsic energy.

Particles are stable condensations of the Spaticle matter substrate

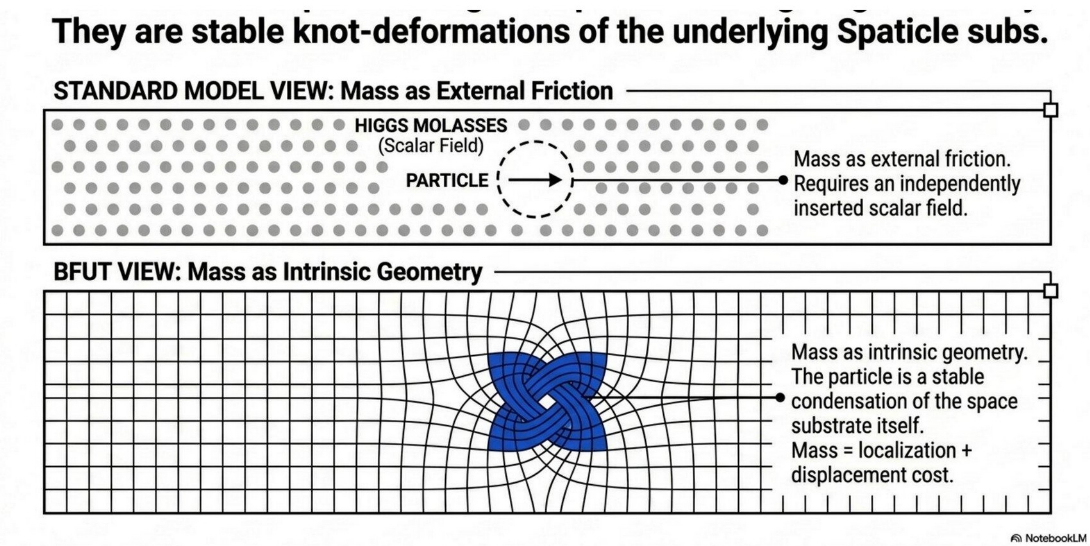

Figure 3: Mass as Intrinsic Geometry, Not External Friction, Standard Model vs BFUT

The H-class state is the electroweak-scale radial resonance of the Spaticle field, not a second field or merely an electroweak projection of another field. The Spaticle field also underlies the gravitational, quantum, confinement, dark-sector and time constructions discussed across the BFUT programme:

Gravity and gravitational carrier dynamics: F1-cov (BFUT P18 [11]) produces the Yukawa gravitational potential with finite domain radii DDR. Galaxy rotation curves across 175 SPARC galaxies are reproduced via the DME equation with rotational entrainment, with shape agreement 92.0% and no dark matter halos (BFUT P18 [11]).

Quantum mechanics: the single-valuedness of $\delta\Psi$ in F1-cov gives $L = n \times \hbar$, the hydrogen energy spectrum, and ground-state selection within the BFUT construction (P19 [10], Section 15).

Strong force and confinement: co-rotating substrate condensations attract by Bernoulli dynamics, producing a linear confinement potential of 0.574 GeV/fm (64% of QCD string tension) with no free parameters (BFUT P16 [1] Section 5B).

Dark matter: BFUT identifies the Spaticle field with the physical substrate used in its dark-sector phenomenology (BFUT P25 [12]).

Time and its arrow: proper time is substrate propagation efficiency. The arrow of time is the irreversibility of substrate propagation. Gravitational time dilation terminates at domain boundaries (BFUT P19 [10] Section 7).

The present paper concerns antimatter, which emerges from the same Spaticle condensation architecture. The H-class radial resonance is one excitation of that single field. The stability filter of Section 6 and the cancellation wave that produces antimatter are substrate-level phenomena and do not depend on the H-class resonance mechanism.

6. The BFUT Account of Antimatter: Stability Filter and Cancellation Wave

The BFUT account of antimatter follows entirely from the stability analysis of P16 [1] (DOI: 10.5281/zenodo.19908215). No new assumptions are introduced. The account has four components.

The stability filter. The Spaticle substrate produces quark-class excitations continuously. The free-energy functional analysis establishes that approximately 97% of parameter space (full five-term functional) produces the stable 3+e topology. These excitations persist as stable quarks, assemble into proton-class and electron-class structures, and form hydrogen. The remaining approximately 3% produces excitations that cannot achieve the geometric balance required for persistence. These are unstable at the individual quark-class level, not at the assembly stage.

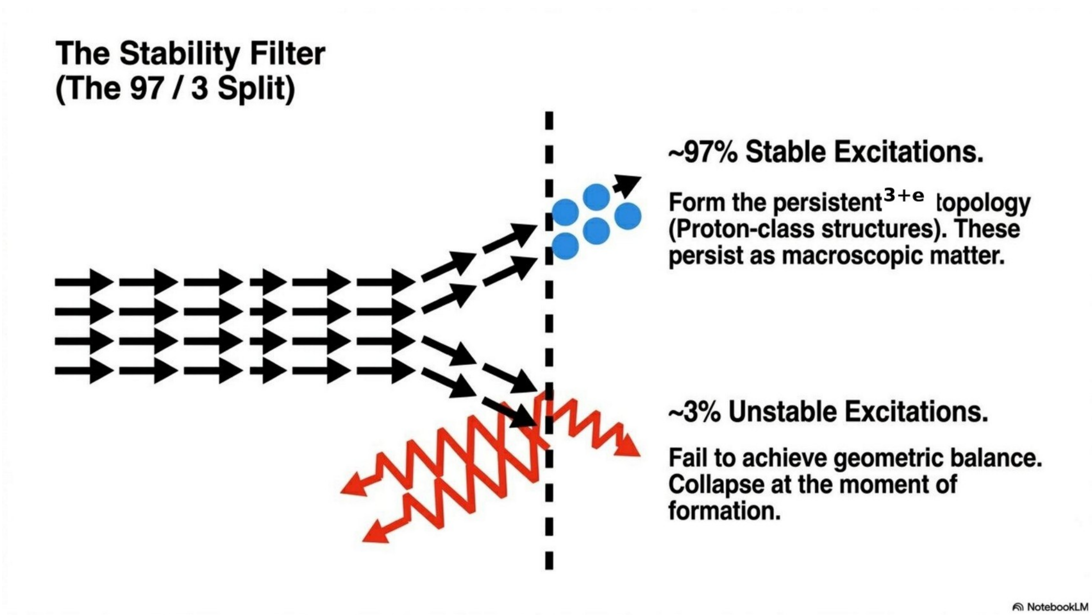

Figure 4: The Stability Filter: 97% stable 3+e topology vs ~3% unstable excitations

The cancellation wave. When an unstable quark-class excitation collapses, the Spaticle substrate generates an equal and opposite rebound deformation in the surrounding medium. This rebound is the antiparticle. It is not an independently generated entity. It is the substrate rebound of the failed excitation. Both cancel simultaneously. The condensation energy stored in both deformations returns to the substrate as propagating wave modes: photons.

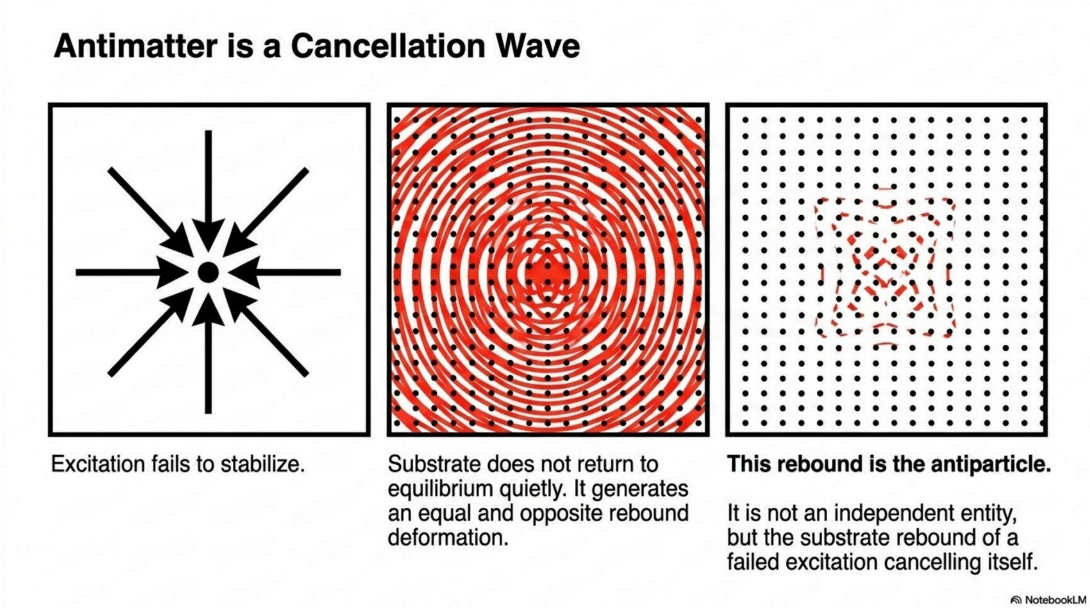

Figure 5: Antimatter as the Cancellation Wave of failed quark-class excitations

Why 100% of mass converts to energy. $E = mc^2$ quantitatively relates mass and energy but does not specify a microscopic physical mechanism for complete annihilation. The BFUT account provides it: the matter deformation and its mirror-image rebound cancel completely. Nothing remains to carry mass. The substrate returns to equilibrium and the stored condensation energy propagates outward into radiation and particle channels; this is the BFUT mechanism proposed for annihilation.

The process is universal and continuous. The stability filter is the permanent operating law of the Spaticle substrate. Wherever and whenever the substrate produces a quark-class excitation, the stability filter operates immediately. The stable fraction persists as matter. Within BFUT, the unstable fraction generates its own cancellation and is proposed to dissolve into propagating excitation modes. This process operates now, everywhere, with no special trigger.

The entire experimental history of particle physics is structurally consistent with the stability-filter result derived from the theoretical parameter scan in P16 [1]. Over seven decades of accelerator operation, laboratories have produced tetraquarks, pentaquarks, exotic heavy resonances, quark-gluon plasma, electroweak bosons, and Higgs bosons. Every one of these is unstable and decays. Across the full experimentally explored energy range, from thermal energies to 13 TeV at the LHC, no confirmed stable alternative to ordinary proton-electron matter has been established. Within BFUT, the 3+e threshold output of P16 [1] is identified as the stable first-threshold quark configuration.

The CERN antihydrogen programme is consistent with this aspect of the BFUT account, but does not directly test the unstable fraction. Within BFUT, antihydrogen is the stable inverse-topology system studied in these experiments and is held under magnetic confinement to prevent contact with matter. Macroscopic stable antimatter has not been produced and stored as bulk material under ordinary conditions; laboratory antihydrogen must be isolated from matter to avoid annihilation. The ordinary substrate environment reflects the stable-topology fraction selected by the stability filter, and the accelerator record confirms that no other stable configuration competes with it.

7. Why the Matter-Antimatter Asymmetry Problem Receives a Different Account in BFUT

The Standard Model does not by itself provide a complete explanation for the observed matter-antimatter asymmetry. BFUT provides a different physical account of this problem.

The asymmetry emerges at the quark-class excitation stability-selection stage. Large stable matter-antimatter populations do not form first. The stable fraction persists as matter. The unstable fraction generates cancellation waves and dissolves as radiation.

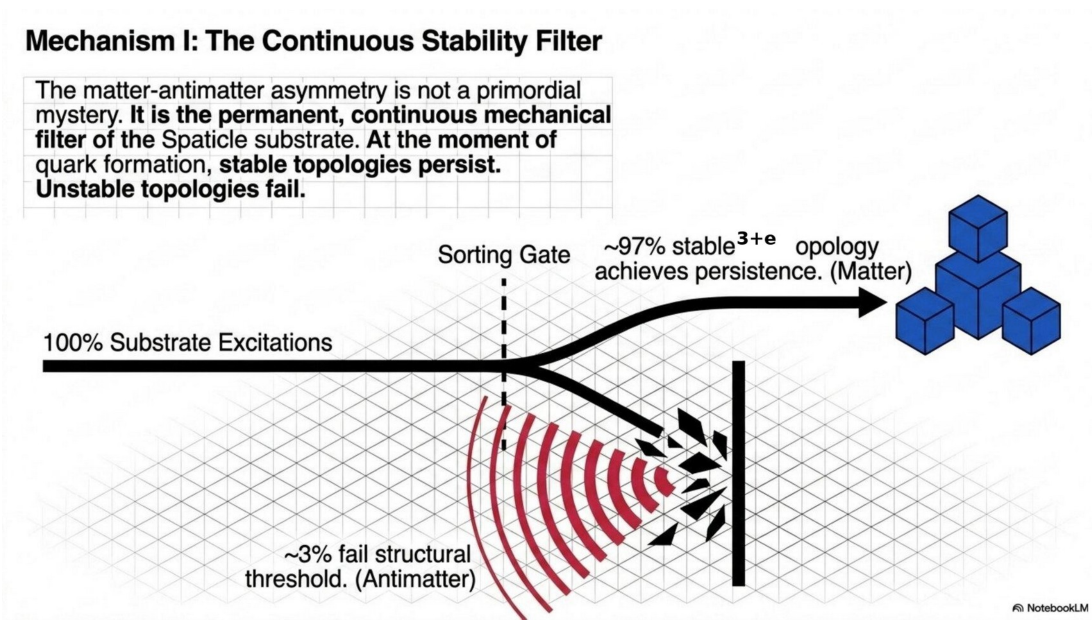

Figure 6: Quark-class excitations forming in the Spaticle substrate

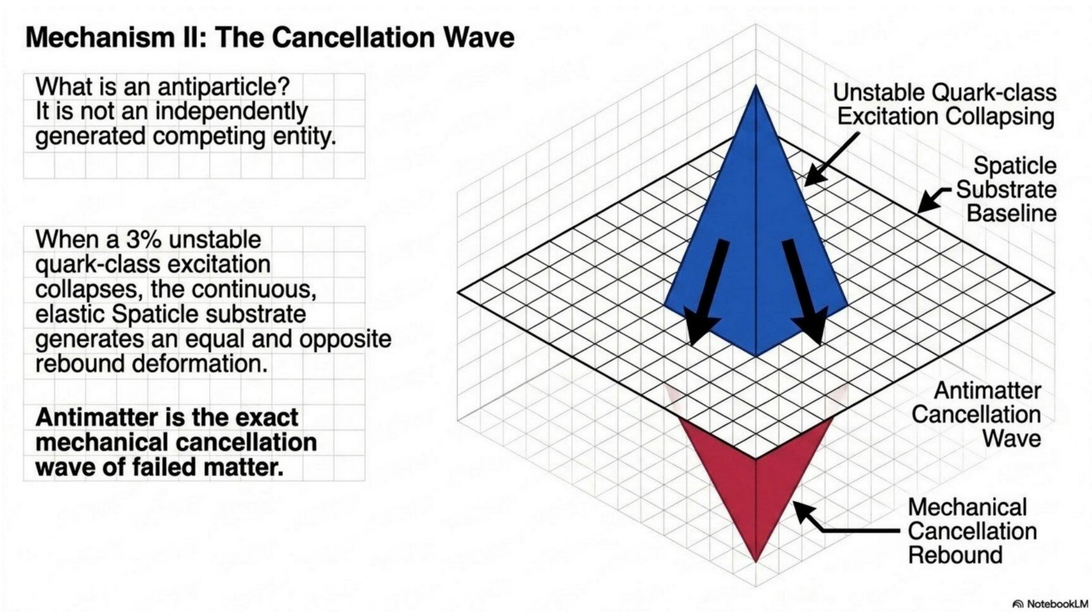

Figure 7: Substrate deformation and cancellation mechanics

The observable universe becomes matter-dominated because only the stable excitation fraction persists macroscopically. No asymmetric initial condition is required. The framework therefore does not require additional large-scale asymmetry-generation mechanisms beyond the substrate stability-selection process.

This mechanism would not be identifiable within the standard antihydrogen spectroscopy programme alone because the relevant dynamics occur at the quark-class excitation formation level, prior to the existence of stable antihydrogen atoms. CERN's antihydrogen programme measures properties of successfully completed inverse topologies. It has no access to the approximately 3% unstable fraction that dissolved at the moment of formation.

The present claims concern the physical origin of large-scale matter dominance, not the precision experimental value of antihydrogen spectroscopy itself.

A further implication of the stability-filter account concerns the Big Bang matter-formation narrative directly. The observed baryon asymmetry is often expressed as roughly one excess baryon per billion baryon-antibaryon pairs [13]. Modern particle physics has revealed that the real configuration space is vastly larger than a simple matter-versus-antimatter binary: tetraquarks, pentaquarks, heavy resonances, quark-gluon plasma states, and dozens of additional hadronic configurations are all physically accessible, yet these excited configurations are unstable and ultimately decay through chains toward stable matter. Within the BFUT framing, the resulting question is why the universe overwhelmingly selected the stable proton-electron hierarchy from a much larger accessible configuration space. The BFUT stability filter provides that mechanism. This argument is developed in full in BFUT P16 [1] Section 10 and in the companion working note "What Particle Physics Actually Shows: The Configuration Space Problem and Its Implications for Big Bang Matter Formation."

8. Four Falsifiable Predictions for the CERN Programme

The four predictions below are experimentally falsifiable. Each includes an explicit falsification condition.

Prediction 1: No CPT violation at any precision. Antihydrogen will be spectroscopically identical to hydrogen. The 1S-2S transition frequency, ground-state hyperfine spectrum, and other spectroscopic properties will match. This follows because the inverse 3+e topology is governed by the same substrate condensation laws and exact mirror geometry. The current agreement will persist as experimental precision improves.

Falsification condition: *A confirmed spectroscopic difference between antihydrogen and hydrogen at any precision level would falsify this prediction and require revision of the BFUT mirror-topology account.*

Prediction 2: Antihydrogen falls at exactly g. Antihydrogen falls downward under gravity at exactly the same acceleration as matter. The weak equivalence principle holds for antimatter exactly. The 2023 ALPHA-g result showed antihydrogen falls downward, consistent with gravitational attraction at approximately 20% precision. BFUT predicts exact equivalence as precision improves. The gravitational behaviour of antihydrogen is identical to hydrogen because the substrate deformation that constitutes gravity acts on both the matter and inverse-matter topology in the same way.

Falsification condition: *A confirmed gravitational acceleration of antihydrogen measurably different from g at any statistically significant precision would falsify this prediction.*

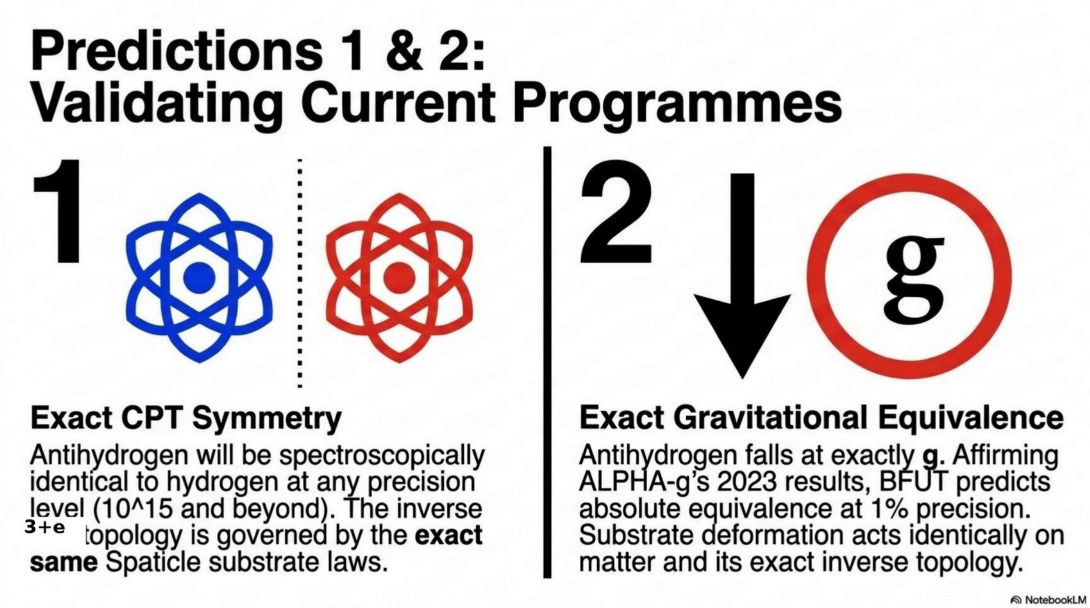

Figure 8: Predictions 1 and 2, Validating Current CERN Programmes

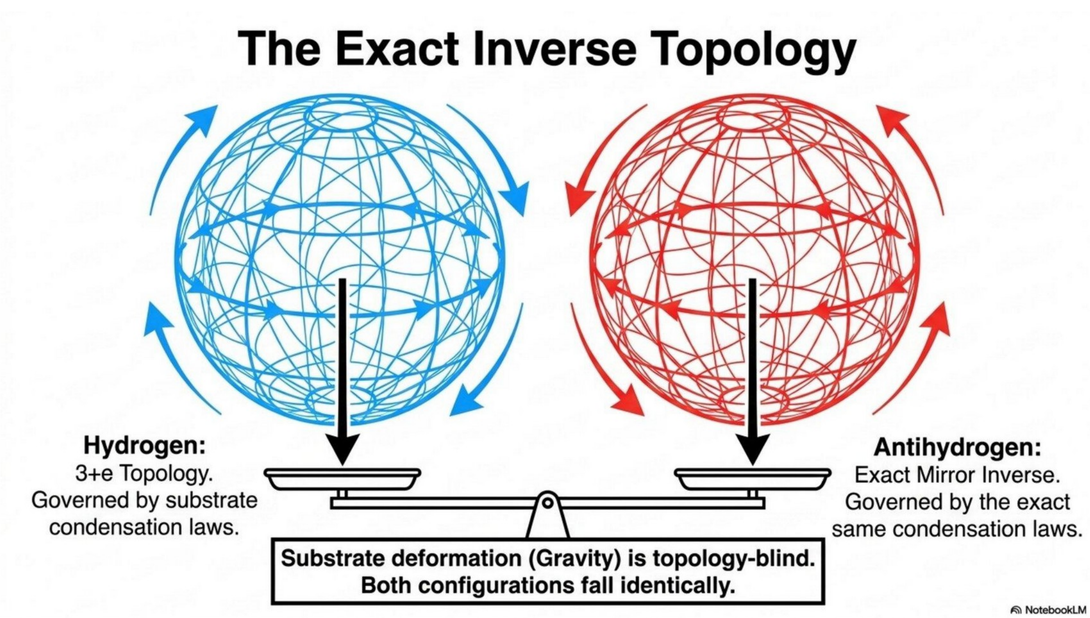

Figure 9: Exact Inverse Topology: Hydrogen vs Antihydrogen

Prediction 3: The asymmetry will not be found in antihydrogen spectroscopy. The matter-antimatter asymmetry of the observable universe will not be found in any property difference between hydrogen and antihydrogen, regardless of the precision achieved. The asymmetry arises from the stability threshold of the Spaticle substrate at the quark-class excitation formation level.

CERN will find perfect symmetry between hydrogen and antihydrogen in all properties they can measure.

Falsification condition: A confirmed property difference between hydrogen and antihydrogen that arises from a fundamental asymmetry in physical law and not from experimental artefact would falsify this prediction.

Prediction 4: Macroscopic stable antimatter domains will not be produced. BFUT predicts that inverse topologies remain difficult to sustain macroscopically because the ordinary substrate environment reflects the stable-topology fraction selected by the stability filter. Any inverse topology excitation in a matter-rich environment will encounter matter and complete its cancellation. The difficulty of producing and storing antihydrogen is consistent with the natural substrate environment already reflecting the stable-topology selection.

Falsification condition: *The production of macroscopic stable antimatter domains stable at ordinary conditions without continuous extreme isolation from matter would falsify this prediction.*

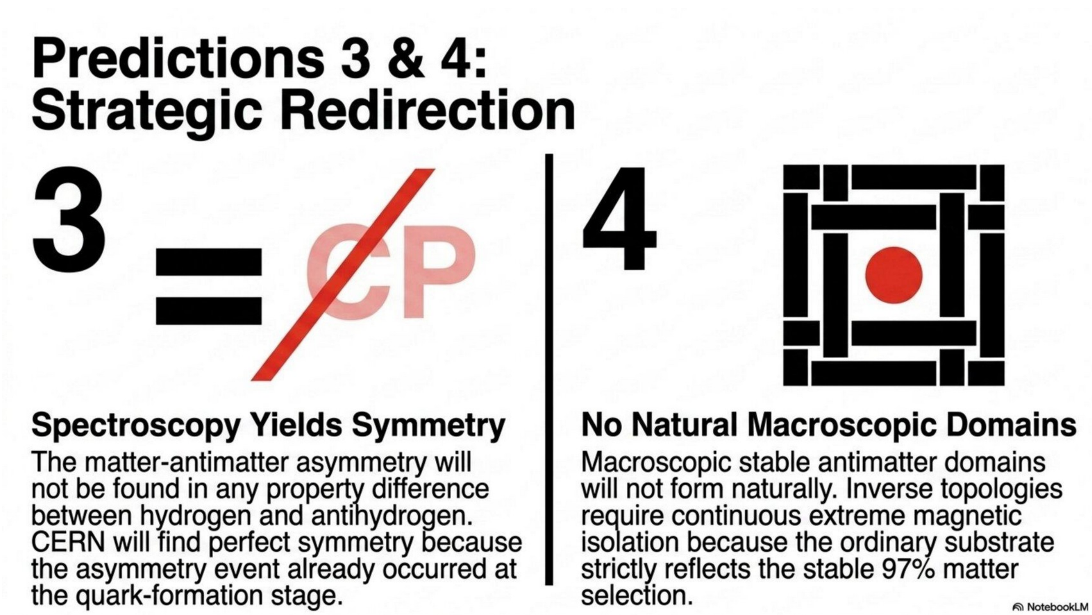

Figure 10: Predictions 3 and 4, Strategic Redirection of the Asymmetry Search

9. What the CERN Programme Does and Does Not Test Within BFUT

The CERN antihydrogen programme is pursuing three goals. Within the BFUT framework, the first two are direct tests of BFUT predictions, while the third is not expected to locate the asymmetry in stable antihydrogen spectroscopy.

CPT testing: supported and important. Testing CPT symmetry between matter and antimatter directly tests a BFUT prediction. BFUT predicts that CPT symmetry will remain consistent at every precision level. The programme is worth pursuing because CPT violation would falsify BFUT as well as the standard model, and because increasingly precise confirmation strengthens the case for exact mirror-topology symmetry.

Equivalence principle testing: supported and important. Directly measuring the gravitational behaviour of antimatter directly tests a BFUT prediction. BFUT predicts exact equivalence. The 2023 result showed antihydrogen falls downward, consistent with ordinary gravitational attraction at the 20% precision achieved; it did not establish equality with g at high precision. Higher precision measurements will directly test this BFUT prediction.

Asymmetry search: BFUT does not expect this route to locate the asymmetry. Within BFUT, the third goal is not expected to be achieved through spectroscopic comparison of hydrogen and antihydrogen. The asymmetry is not located in any property of stable antihydrogen atoms. It is located in the stability threshold of the Spaticle substrate at the quark-class excitation formation level. The CERN programme produces and measures stable antihydrogen, the successfully completed inverse-topology fraction. It has no access to the approximately 3% unstable fraction that dissolved at the moment of formation.

Diagnostic Paradigm Shift: Standard Model vs. BFUT

CPT Symmetry	Standard Model: Postulated mathematically.	**Exact Mirror Topology.** Inverse topologies obey identical substrate condensation laws.
Gravity on Antimatter	Standard Model: Assumed via CPT.	**Topology-Blind Deformation.** Gravity acts identically on matter and inverse-matter topology.
Cosmological Asymmetry	Standard Model: Assumed large symmetric populations followed by unknown CP-violation.	**Stability Filter at Formation.** Asymmetry originates at the individual quark excitation stage.

NotebookLM

Figure 11: Diagnostic Paradigm Shift: Standard Model vs BFUT

This is not a criticism of the CERN programme. The experimental work on CPT symmetry and the equivalence principle is of the highest scientific value. The point is that the third goal requires a different experimental approach: studying the substrate dynamics of quark-class excitation formation, which is a different experimental target from stable antihydrogen spectroscopy.

The Standard Model describes ordinary-matter stability and exotic-state instability through quantum chromodynamics, confinement, gauge symmetries, conservation laws, spontaneous symmetry breaking, and effective field treatments. BFUT derives the hierarchy from one substrate stability-selection process. In the BFUT account, the asymmetry originates at quark-class formation and is not encoded in the properties of stable antihydrogen.

Within the Standard Model, electroweak symmetry breaking and high-energy scattering consistency use a scalar vacuum field. BFUT derives the corresponding electroweak structures from substrate condensation mechanics. The same stability-selection process then determines both the hierarchy and the asymmetry.

10. The Physical Explanation of Annihilation Energy

Matter-antimatter annihilation converts the total rest-energy of the annihilating system into other particle and radiation channels. Fusion releases about 0.7% of the reacting rest mass. $E = mc^2$ states the energy relation; the BFUT account supplies its proposed substrate mechanism.

The matter particle and the antiparticle are equal and opposite substrate deformations. When the two meet, the original excitation and its mirror image cancel identically. Nothing is left to carry mass because the cancellation is geometrically exact. Within the BFUT mechanism, the substrate returns to its equilibrium state and the stored energy propagates outward into radiation and particle channels; this describes the BFUT annihilation mechanism specifically, not every experimentally observed annihilation final state.

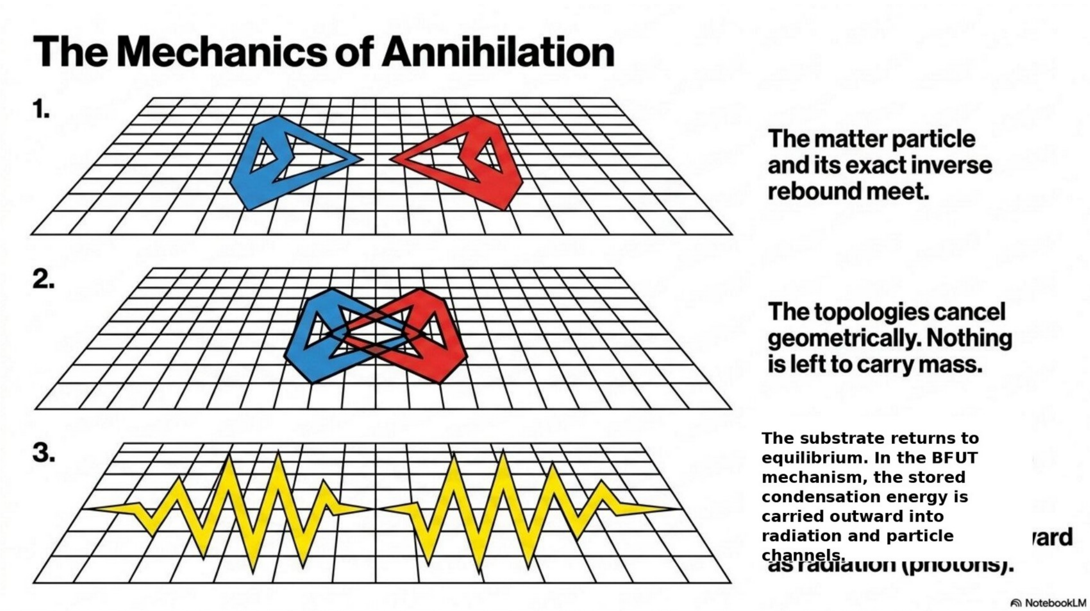

Figure 12: Total Topological Annihilation: Exact geometric cancellation

Nuclear fission releases about 0.1% of the initial rest mass and hydrogen fusion about 0.7%. In the BFUT annihilation mechanism, the excitation and its exact mirror deformation cancel completely, so no rest-mass-bearing remnant of that pair remains.

Antimatter is therefore difficult to produce, isolate, and store as an energy source. CERN reports that accelerator production is extremely small and that production requires far more energy than the stored antimatter can release [15].

11. Consistency with the Full BFUT Framework

The antimatter account in the present paper is a direct consequence of the stability analysis already established in P16 [1]. P16 [1] establishes the 3+e condensation topology as the unique stable output of the substrate threshold analysis. P17 [8] derives the four fundamental forces from that topology, including the electromagnetic force from the internal circulation asymmetry that distinguishes the proton-class charge +1 from the electron-class charge -1. The exact mirror symmetry of the inverse topology that produces antiparticles is therefore a consequence of the same circulation analysis that produces charge in the first place.

P19 [10] applies the P16 [1] condensation structure to particle couplings and resonances. For the charged sector, P16 supplies $M = m_p/3$ and $n^2 = 16$; P19 then obtains m_W_vss = 256M. The neutral core-stay resonance gives m_Z_vss = $\pi^4 m_p$ independently. The mixing quantity is consequently an output, $\sin^2\theta$_W_vss = 1 − (m_W_vss/m_Z_vss)^2 = 0.23257.

The Standard Model distributes these phenomena across confinement, gauge symmetry, spontaneous symmetry breaking, and Higgs-sector interactions. BFUT treats them as consequences of a unified Spaticle-field condensation structure. In this account, the observed H-class resonance is the electroweak-normalised radial resonance of that single field.

BFUT Paper 18 [11] defines the deformation radius $R_d = [3M/(8\pi\rho_s)]^{1/3}$ and the rotationally extended radius $R_{eff} = R_d(1 + v\_rot^2/c^2)^{1/3}$. The equilibrium density ρ_s governs the gravitational-domain construction. Rotational entrainment generates the additional outer-galaxy gravitational support.

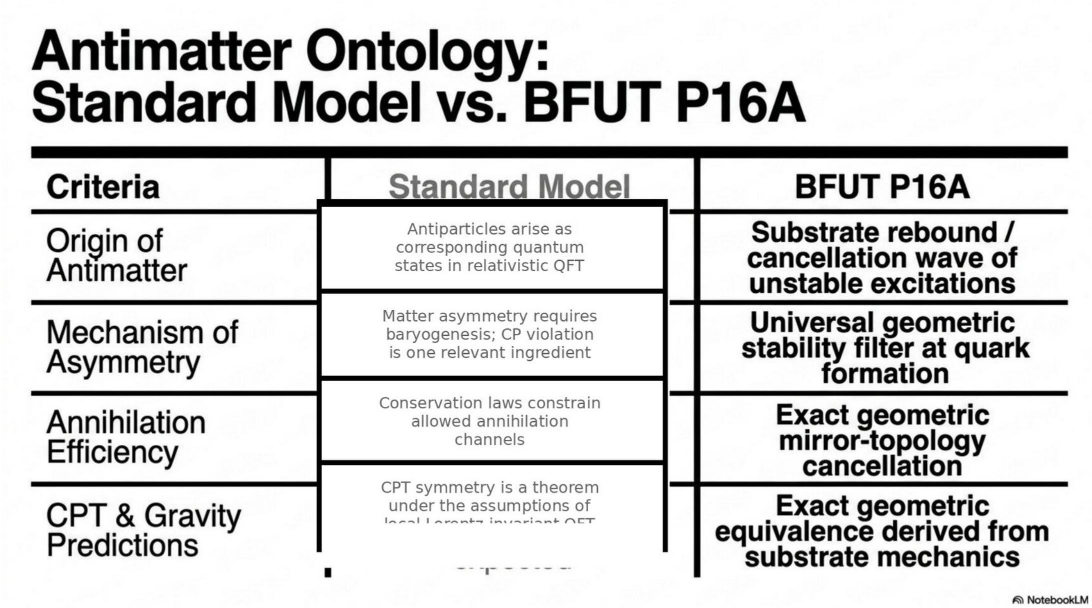

Figure 13: Antimatter Ontology, Standard Model vs BFUT P16A

12. Conclusion

The CERN antihydrogen programme is pursuing three scientific goals. The BFUT framework supports two of them fully and predicts their outcome: CPT symmetry will be confirmed at every precision level, and antihydrogen will be found to fall under gravity identically to matter. The third goal will not achieve its objective through spectroscopic comparison of stable antihydrogen to hydrogen, because the asymmetry is not located in any property of stable antihydrogen.

The BFUT account provides a different physical account of the matter-antimatter asymmetry problem without requiring any new physics beyond the stability analysis of P16 [1]. The approximately 97% of quark-class excitation parameter space that achieves stable 3+e topology persists as matter. The remaining approximately 3% that cannot stabilise generates its own cancellation wave and dissolves as radiation at the moment of formation. The observable universe becomes matter-dominated because only the stable excitation fraction persists macroscopically.

The four predictions stated in Section 8 are specific, quantitative, and falsifiable. They precede any further CERN data and will be confirmed or falsified by the ongoing experimental programme. A continuing experimental target is improvement beyond the 2023 gravitational precision, with 1% precision among the goals of CERN antihydrogen-gravity programmes. The BFUT prediction remains exact equivalence at every precision level.

The stability-filter prediction at the core of this paper is structurally consistent with the full particle physics experimental record, not only with the CERN antihydrogen results specifically. Across all experimentally explored accelerator energies, no confirmed stable matter configuration outside the ordinary proton-electron hierarchy has been established. The BFUT framework derives this observed hierarchy from a single substrate-level stability-selection principle. The four predictions stated in this paper are therefore grounded in a framework whose stability account is consistent with the broadest available experimental base.

The CERN antihydrogen predictions are one experimental test of the same substrate condensation framework used for the stability filter, particle relations, and gravitational dynamics.

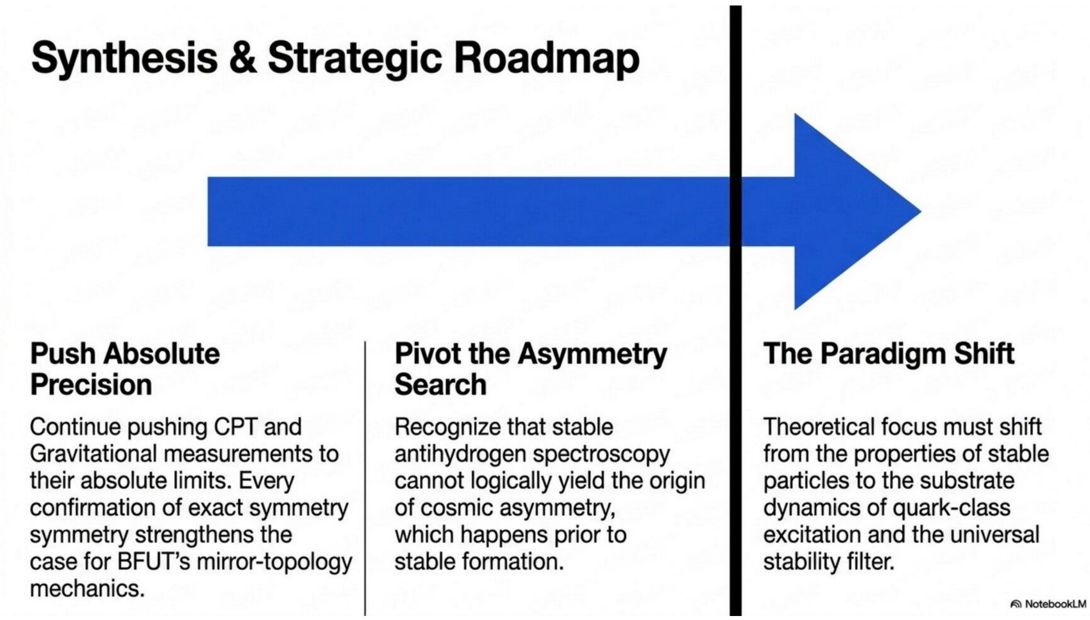

Figure 14: Synthesis and Strategic Roadmap

13. References

[1] Sharma, V. S. (2026). The Origin of Matter, Antimatter, and Fundamental Forces: How Protons, Electrons, and Hydrogen Formed. BFUT P16. Zenodo. DOI: 10.5281/zenodo.19908215

[2] Sharma, V. S. (2026). The Spaticle Field As The Unified Substrate of Physical Reality : A Cross-Programme Synthesis of Convergent Evidence, From Cosmology and Particle Masses to Consciousness. BFUT P14. Zenodo. DOI: 10.5281/zenodo.19394064

[3] Sharma, V. S. (2026). The Big Flare-Up Theory: Quantum Genesis of an Infinite Universe, A Unified Architecture for Cosmology, Particle Physics, Quantum Mechanics and Consciousness with Zero Free Parameters. BFUT L1. Zenodo. DOI: 10.5281/zenodo.19149785

[4] Borchert, M. J., et al. (BASE Collaboration). (2022). A 16-parts-per-trillion measurement of the antiproton-to-proton charge–mass ratio. Nature, 601, 53–57. DOI: 10.1038/s41586-021-04203-w

[5] Ahmadi, M., et al. (ALPHA Collaboration). (2018). Characterization of the 1S–2S transition in antihydrogen. Nature, 557, 71–75. DOI: 10.1038/s41586-018-0017-2

[6] Amole, C., et al. (ALPHA Collaboration). (2012). Observation of the hyperfine spectrum of antihydrogen. Nature, 483, 439–443. DOI: 10.1038/nature10942

[7] ALPHA Collaboration. (2023). Observation of the effect of gravity on the motion of antimatter. Nature, 621, 711–716. DOI: 10.1038/s41586-023-06527-1

[8] Sharma, V. S. (2026). The Emergence of Forces and Fundamental Senses: How the Spaticle Field Gave Rise to Gravity and All Other Forces. BFUT P17. Zenodo. DOI: 10.5281/zenodo.19976408

[9] Sharma, V. S. (2026). Unifying Quantum Mechanics with Gravity, Demystifying Twenty Quantum Phenomena Including Half-Integer Spin, the Born Rule, Wave Function Collapse, and Higgs Physics. BFUT P19A. Zenodo. DOI: 10.5281/zenodo.20145695

[10] Sharma, V. S. (2026). Unification of Particle Physics: Deriving Fine Structure and Coupling Constants, W, Z, and Higgs Boson Masses, Redefining and Unifying Gravity and Time. BFUT P19. Zenodo. DOI: 10.5281/zenodo.20145567

[11] Sharma, V. S. (2026). Beyond General Relativity: A Unified Gravitation Equation Across Quantum, Classical, Galactic, and Rapid-Transition Regimes. BFUT P18. Zenodo. DOI: 10.5281/zenodo.20145506

[12] Sharma, V. S. (2026). Dark Matter: Connecting Galaxy Clusters, Galaxy Rotations, the Cosmological Constant, W and Z Boson Masses, and Atomic Structure Through One Physical Constant. BFUT P25. Zenodo. DOI: 10.5281/zenodo.20535295

[13] Canetti, L., Drewes, M., & Shaposhnikov, M. (2012). Matter and antimatter in the universe. New Journal of Physics, 14, 095012. DOI: 10.1088/1367-2630/14/9/095012

[14] Baker, C. J., et al. (ALPHA Collaboration). (2025). Precision spectroscopy of the hyperfine components of the 1S-2S transition in antihydrogen. Nature Physics. DOI: 10.1038/s41567-024-02712-9

[15] CERN. Antimatter: FAQ and production scale of accelerator antiprotons. CERN public information. https://home.cern/science/physics/antimatter

[16] Akbari, R., et al. (ALPHA Collaboration). (2026). Four ppm measurement of the antihydrogen ground-state hyperfine splitting. Nature, 653, 1022–1026. DOI: 10.1038/s41586-026-10556-x

[17] Navas, S., et al. (Particle Data Group). (2024). Review of Particle Physics. Physical Review D, 110, 030001; 2025 update.